PHYSICAL REVIEW A **85**, 023415 (2012)

Anticrossing-mediated entanglement of adsorbed polar molecules

Ying-Yen Liao[*]
Department of Applied Physics, National University of Kaohsiung, Kaohsiung 811, Taiwan

(Received 17 August 2011; published 21 February 2012)

We study the entanglement of two adsorbed polar molecules in static electric fields. The concurrence is estimated to quantify the entanglement. The adsorbed molecules reveal significant rotational characteristics, such as anticrossing features, due to the influences of electric field and quantum confinement. Numerical results demonstrate that these rotational properties dominate the amount and profile of concurrence. At zero temperature, an enhanced concurrence is obtained near the anticrossing in the ground state. Moreover, we analyze the effect of temperature on the concurrence. The temperature-dependent concurrence displays a suppressed behavior, especially at the anticrossing.

DOI: 10.1103/PhysRevA.85.023415 PACS number(s): 33.80.Be, 33.20.Sn, 34.35.+a, 03.67.Bg

I. INTRODUCTION

The development of exploring entanglement has opened up a variety of exciting research opportunities [1]. Entanglement is a nonclassical property that represents a correlation between two or more quantum systems [2]. For instance, the quantum state of two entangled states cannot be regarded as a product of the individual quantum states. Such a quantum mechanical feature has been surveyed in a variety of physical systems ranging from atoms to quantum dots [3,4]. The implementation of entanglement is further oriented toward applications of quantum computation and quantum information [5]. In addition to these platforms, polar molecules have recently become one of the best prototypes for exploring entanglement [6–8]. Polar molecules display prosperous perspectives in view of their internal properties and interactions [9,10]. Molecular parameters, such as energy levels and wave functions, can be flexibly modified via external electric fields. Such a tunability is derived from the coupling of the field to dipole moment [11,12]. Consequently, it is absolutely useful to manipulate the molecular properties through external influence for probing entanglement in polar molecules.

A basic scheme consisting of coupled polar molecules can generate entanglement [13,14]. One of the generating sources originates from the dipole-dipole interaction [15]. The parameters of the interaction, such as its strength, affect the degree of entanglement. To explore molecular entanglement, recent work has undertaken the study of coupled polar molecular systems that are subject to lasers or static electric fields [7,8]. The dressed rotational states under external fields are addressed with the help of a free rotor model. Compared with efforts in free molecules, however, exploration of the entanglement of adsorbed polar molecules is still lacking. The rotational motion of the adsorbed molecule is hindered and different from that of a free rotor [16] because the rotational properties are strongly affected by the interaction between the molecule and its surrounding environment [17,18]. In order to study these molecules in depth, we aim to investigate the influence of the hindered rotation on the entanglement of adsorbed molecules, especially in electric fields. The electric field allows one to tailor the rotational states of the molecules. Therefore, the entanglement will become interesting in the system.

In this work, we investigate the entanglement of two adsorbed polar molecules that will become important in a static electric field. The method of exact diagonalization is applied to evaluate the effect of an electric field on the rotational states. By tuning the electric field, adsorbed molecules markedly reveal anticrossing features between energy levels. We further employ the concurrence to measure the entanglement of the system. An enhanced behavior is obtained at zero temperature. The results of the excited states are discussed as well. Furthermore, we analyze the dependence of temperature on the concurrence. The concurrence at the anticrossing is suppressed with increase of temperature.

The paper is organized as follows. In Sec. II we describe the theoretical model and the method of calculation for confined molecules. In Sec. III we exhibit the results of numerical calculations in detail, including energy states and concurrence. The related comparison and discussion are interpreted in Sec. IV. Finally, there is a conclusion in Sec. V.

II. MODEL SYSTEM

A. Hamiltonian

We consider two polar diatomic molecules that are solidly adsorbed on a surface. Both molecules are identical and spatially separated by a distance d. For each molecule, its rotational motion is hindered by a surface potential, as illustrated in Fig. 1. A conical well with finite barriers is proposed to depict the surface potential [19]. The geometry of potential is assumed to be symmetric with respect to the z axis, i.e., the structure of the well is independent of the azimuthal angle [17,19]. The conical well is then partitioned into two regions with different potential barriers. In such confinement, the molecular rotation demonstrates particular features. To flexibly control the rotational properties of the molecules, a static electric field is externally applied along the z axis. The Hamiltonian for coupled adsorbed molecules is then expressed as

$$H = \sum_{i=1}^{2} \left(B\mathbf{J}_i^2 + V_c^i + V_e^i \right) + V_d, \tag{1}$$

---

[*] yyliao@nuk.edu.tw

where B is the rotational constant and $\mathbf{J}_i$ is the rotational angular-momentum operator. The notation $i = 1$ and 2 represents the left and right molecules, respectively. The conical well V_c^i is given by

$$V_c^i = \begin{cases} 0, & 0 \leqslant \theta_i \leqslant \alpha \\ V_0, & \alpha < \theta_i \leqslant \pi \end{cases} \tag{2}$$

where α is the hindrance angle and V_0 is the barrier height. The coupling of a dipole moment μ with a static electric field ϵ along the z axis is written as

$$V_e^i = -\omega \cos\theta_i, \tag{3}$$

where $\omega = \mu\epsilon$ is the field strength parameter. According to the molecular positions indicated by the coordinates, one can derive the interaction between two electric dipoles [7]. Since two dipoles are separated by a vector $\mathbf{d} = d\hat{\mathbf{y}}$, the dipole-dipole interaction V_d is simplified to be

$$\begin{aligned} V_d = {} & U_0(-2\sin\theta_1 \sin\phi_1 \sin\theta_2 \sin\phi_2 \\ & + \sin\theta_1 \cos\phi_1 \sin\theta_2 \cos\phi_2 + \cos\theta_1 \cos\theta_2), \end{aligned} \tag{4}$$

with $U_0 = \mu^2/4\pi\varepsilon_0 d^3$ the interaction strength parameter and ε_0 the permittivity of free space.

B. Method

For a single adsorbed polar molecule in the electric field, the energy $\varepsilon_{\sigma,m}$ and its wave function $\Psi_{\sigma,m}$ for the (σ,m) energy state can be obtained by solving the Schrödinger equation (i omitted)

$$(B\mathbf{J}^2 + V_c + V_e)\Psi_{\sigma,m} = \varepsilon_{\sigma,m}\Psi_{\sigma,m}, \tag{5}$$

where $\Psi_{\sigma,m}$ is a superposition of a suitably large basis set which is formed from the field-free eigenfunctions $\psi_{l,m}$ of single adsorbed-molecule model [19]. Here the wave function $\psi_{l,m}$ with quantum number (l,m) reads

$$\psi_{l,m}(\theta,\phi) = \begin{cases} A^{\mathrm{I}}_{l,m} P_{\mathrm{I}}\left(\upsilon^{\mathrm{I}}_{l,m}, m, \cos\theta\right)\exp(im\phi), & 0 \leqslant \theta \leqslant \alpha \\ A^{\mathrm{II}}_{l,m} P_{\mathrm{II}}\left(\upsilon^{\mathrm{II}}_{l,m}, m, \cos\theta\right)\exp(im\phi), & \alpha < \theta \leqslant \pi \end{cases} \tag{6}$$

with

$$P_{\mathrm{I}}\left(\upsilon^{\mathrm{I}}_{l,m}, m, \cos\theta\right) = \sin^{|m|}\theta\, F\left(|m| - \upsilon^{\mathrm{I}}_{l,m}, 1 + |m| + \upsilon^{\mathrm{I}}_{l,m}, 1 + |m|\,; \frac{1-\cos\theta}{2}\right) \tag{7}$$

and

$$P_{\mathrm{II}}\left(\upsilon^{\mathrm{II}}_{l,m}, m, \cos\theta\right) = \sin^{|m|}\theta\, F\left(|m| - \upsilon^{\mathrm{II}}_{l,m}, 1 + |m| + \upsilon^{\mathrm{II}}_{l,m}, 1 + |m|\,; \frac{1+\cos\theta}{2}\right), \tag{8}$$

where F represents the hypergeometric function [20]. $A^{\mathrm{I}}_{l,m}$ and $A^{\mathrm{II}}_{l,m}$ are the normalization constants. The notation system I and II is used for the two regions. By matching the boundary conditions at the angle α, one can obtain the values of positive numbers $\upsilon^{\mathrm{I}}_{l,m}$ and $\upsilon^{\mathrm{II}}_{l,m}$ from the following equation:

$$P_{\mathrm{I}}\left(\upsilon^{\mathrm{I}}_{l,m}, m, \cos\alpha\right) P'_{\mathrm{II}}\left(\upsilon^{\mathrm{II}}_{l,m}, m, \cos\alpha\right) - P'_{\mathrm{I}}\left(\upsilon^{\mathrm{I}}_{l,m}, m, \cos\alpha\right) P_{\mathrm{II}}\left(\upsilon^{\mathrm{II}}_{l,m}, m, \cos\alpha\right) = 0, \tag{9}$$

with $P'_{\mathrm{I}} = dP_{\mathrm{I}}/d\theta$, $P'_{\mathrm{II}} = dP_{\mathrm{II}}/d\theta$, and $\upsilon^{\mathrm{II}}_{l,m}(\upsilon^{\mathrm{II}}_{l,m} + 1)B = \upsilon^{\mathrm{I}}_{l,m}(\upsilon^{\mathrm{I}}_{l,m} + 1)B - V_0$.

The effect of the dipole-dipole interaction on coupled adsorbed molecules can be analyzed with the help of the above results. For each adsorbed molecule, the system decreases to a two-level system with the ground state $|0\rangle = |\sigma = 0, m = 0\rangle$ and the first excited state $|1\rangle = |\sigma = 1, m = 0\rangle$, corresponding to the energies $\varepsilon_0 = \varepsilon_{0,0}$ and $\varepsilon_1 = \varepsilon_{1,0}$, respectively. By restoring the marked numbers in subscript, the basis states $|00\rangle = |0_1\rangle \otimes |0_2\rangle$, $|01\rangle = |0_1\rangle \otimes |1_2\rangle$, $|10\rangle = |1_1\rangle \otimes |0_2\rangle$, and $|11\rangle = |1_1\rangle \otimes |1_2\rangle$ are built to solve the Hamiltonian in Eq. (1). The eigenvalues E_j and their corresponding eigenfunctions Φ_j are obtained by diagonalizing the matrix in the basis

$$\tilde{H} = \begin{pmatrix} 2\varepsilon_0 + \Omega_{0,0} & \Omega_{0,2} & \Omega_{0,2} & \Omega_{2,2} \\ \Omega_{0,2} & \varepsilon_0 + \varepsilon_1 + \Omega_{0,1} & \Omega_{2,2} & \Omega_{1,2} \\ \Omega_{0,2} & \Omega_{2,2} & \varepsilon_0 + \varepsilon_1 + \Omega_{0,1} & \Omega_{1,2} \\ \Omega_{2,2} & \Omega_{1,2} & \Omega_{1,2} & 2\varepsilon_1 + \Omega_{1,1} \end{pmatrix}, \tag{10}$$

with $\Omega_{\alpha,\beta} = U_0\Gamma_\alpha\Gamma_\beta$ consisting of the factors $\Gamma_0 = \langle 0_i\,|\cos\theta_i|\,0_i\rangle$, $\Gamma_1 = \langle 1_i\,|\cos\theta_i|\,1_i\rangle$, and $\Gamma_2 = \langle 1_i\,|\cos\theta_i|\,0_i\rangle$ for $i = 1$ and 2. It is worth mentioning that $\Omega_{\alpha,\beta}$ are not related to the azimuthal angle. The results come from the fixed quantum number $m = 0$ so that the first and second parts of V_d in Eq. (4) average to zero [8].

C. Concurrence

Next, the entanglement of adsorbed molecules is explored by employing the density matrix method [21]. At temperature T, the density matrix generally reads $\rho = \exp(-H/k_B T)/Z$ with the Boltzmann constant k_B and partition function

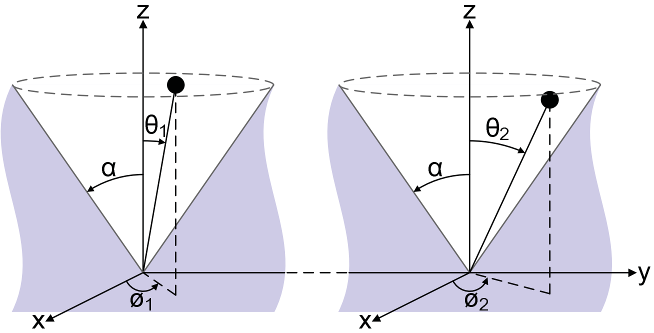

FIG. 1. (Color online) Two identical conical wells with hindrance angles α. Each well consists of two distinct potential barriers, differentiated by the hindrance angle. The left and right molecules are located at $(x,y,z) = (0,0,0)$ and $(0,d,0)$, respectively. Their moments of inertia are marked by the filled circles.

$Z = \mathrm{Tr}[\exp(-H/k_BT)]$ [22]. In the model, the corresponding density matrix is clearly described as

$$\rho(T) = \frac{1}{Z}\sum_{j=1}^{4}\exp(-E_j/k_BT)|\Phi_j\rangle\langle\Phi_j|, \tag{11}$$

with

$$Z = \sum_{j=1}^{4}\exp(-E_j/k_BT). \tag{12}$$

Based on the density matrix, one can use the concurrence C to measure the entanglement of the molecular system. The concurrence is then defined as

$$C = \max\{0, \lambda_1 - \lambda_2 - \lambda_3 - \lambda_4\}, \tag{13}$$

where $\{\lambda_k\}$ are the square roots of the eigenvalues in decreasing order of the matrix

$$\varrho = \rho(\sigma_y \otimes \sigma_y)\rho^*(\sigma_y \otimes \sigma_y), \tag{14}$$

where σ_y is the Pauli matrix and ρ^* is the complex conjugate of ρ. The concurrence ranges from $C = 0$ for nonentangled states to $C = 1$ for the maximum degree of entanglement.

III. NUMERICAL RESULTS

The single-molecule system is analyzed to characterize the rotational properties. Calculations are performed for a barrier height $V_0/B = 50$ and a hindrance angle $\alpha = 40^\circ$. Figure 2(a) shows the rotational-state energies of a single adsorbed polar molecule for fixed quantum number $m = 0$. The coupling of the dipole moment with the electric field induces level shifts. The energies generally diminish with increasing field strength. In particular, the anticrossing features between the energy levels are observed in the case of $\omega < 0$. The adjacent energy levels do not cross each other due to the same quantum number m. The energy levels with $m \neq 0$ show similar behavior. For the lowest energy, one can clearly see an anticrossing between the $(\sigma,m) = (0,0)$ and $(1,0)$ energy levels at the point $\omega^*/B \simeq -25.474$. The surrounding region is enlarged in the inset of Fig. 2(a). The energy gap between the two states is $\Delta^*/B \simeq 7.7 \times 10^{-3}$. Such an anticrossing feature originates from the presence of the conical well. For $\omega > \omega^*$, the influence of quantum confinement is stronger than that of the electric field. As illustrated in Fig. 2(b), the probability density $|\Psi_{0,0}|^2$ of the ground state is mostly located inside the well while the probability density $|\Psi_{1,0}|^2$ of the first excited state spreads outside the well. When the strength of the electric field increases sufficiently strongly, the adsorbed molecule will be pushed to overcome the confinement of the hindered potential. The consequence leads to a drastic transformation in the distribution of the two states in the case of $\omega < \omega^*$ [see Fig. 2(c)].

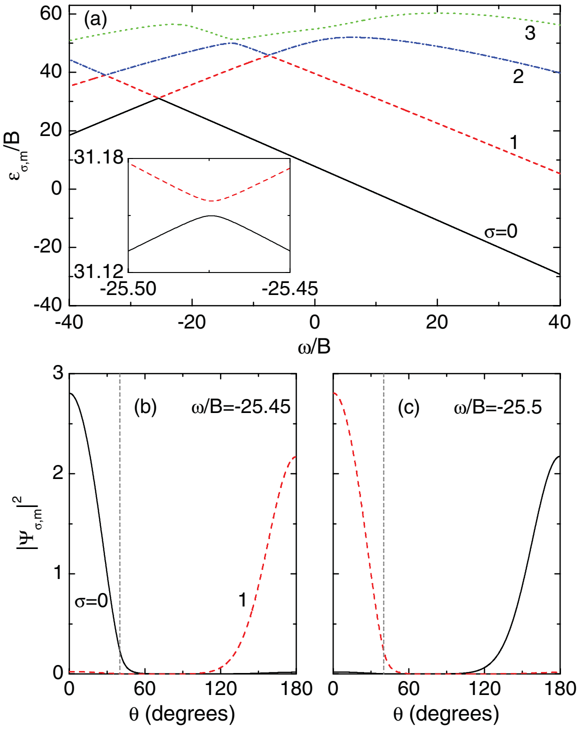

FIG. 2. (Color online) (a) Low-lying energy spectrum as a function of field strength parameter for $m = 0$. The inset emphatically shows an anticrossing between the $(\sigma,m) = (0,0)$ and $(1,0)$ energy states. (b) and (c) represent the probability densities of the (0,0) and (1,0) energy states for $\omega/B = -25.45$ and -25.5, respectively. The dotted gray line denotes the hindrance angle $\alpha = 40^\circ$.

Let us now examine the entanglement of coupled polar molecules. The related properties closely rely on the temperature and rotational states as shown in Eq. (11). In such a limit of $T = 0$ K, the ground state $|\Phi_1\rangle$ plays a dominant role in the entanglement of the system. Figure 3 shows the concurrence for different interaction strength parameters U_0. The electric field is applied around the region, where the anticrossing exhibits in the ground state of a single adsorbed molecule [see the inset of Fig. 2(a)]. For a fixed U_0, the concurrence reveals an enhanced behavior, depending on the strength of the electric field. Its value reaches a maximum at the anticrossing point ω^* corresponding to a highly entangled system. For instance, the concurrence approaches 0.71 in the case of $U_0/B = 0.01$. Once the electric field is tuned away from the region, however, the concurrence will drop rapidly to a small value. At $\omega/B = -25.4$, the concurrence for $U_0/B = 0.01$ is as low as 2.7×10^{-4}. Actually, the concurrence is slight in the case of $\omega > 0$. Up to several orders

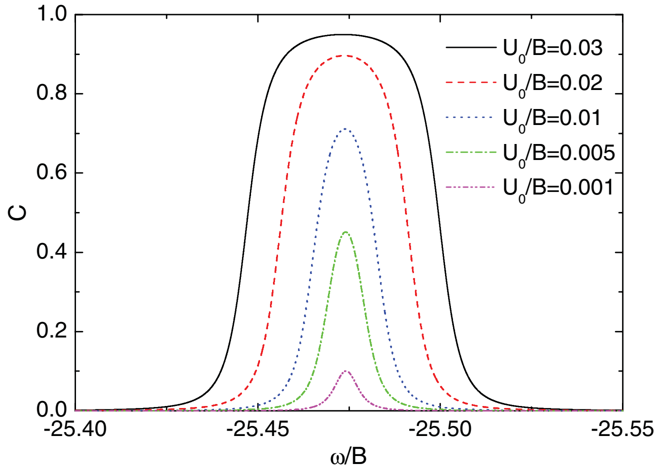

FIG. 3. (Color online) Concurrence for different interaction strength parameters. The electric field is tuned over the region of anticrossing in the ground state of a single adsorbed polar molecule. The temperature is $T = 0$ K.

of magnitude variation of the concurrence are achieved by tuning the electric field. Furthermore, increasing the parameter U_0 would strengthen the dipole-dipole interaction. A stronger correlation between two molecules leads to an increase in the concurrence. Consequently, one can control the features of entanglement by tuning the parameters of the system.

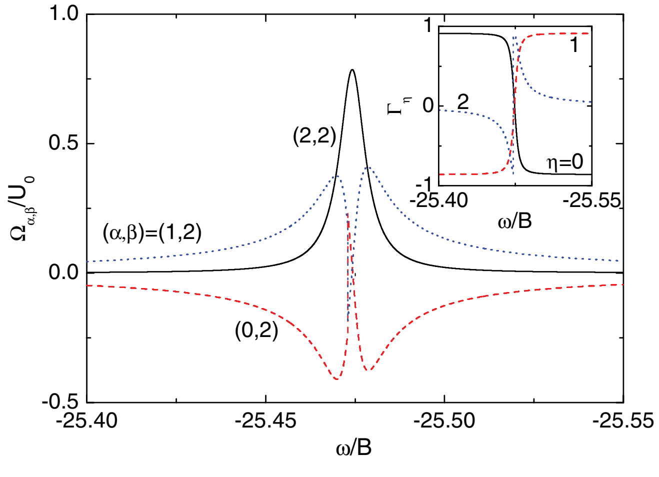

FIG. 4. (Color online) Off-diagonal elements as a function of field strength parameter. The inset shows the factors Γ_η for $\eta = 0$, 1, and 2.

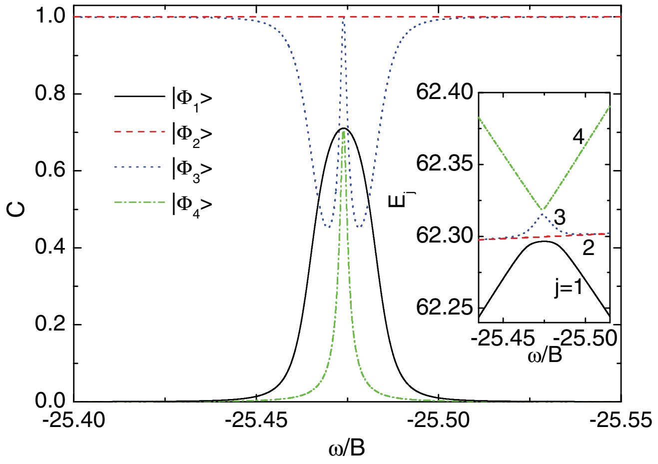

FIG. 5. (Color online) Concurrences of the four states for $U_0/B = 0.01$. The inset partially shows the corresponding energies of the four states.

To capture the enhanced feature, one can analyze the elements of the matrix shown in Eq. (10). The influence of the off-diagonal elements is critical to induce the entanglement via the dipole-dipole interaction. Due to the symmetry, merely three different components contribute effect to the off-diagonal part of the matrix. From Fig. 4, the elements obviously exhibit drastic fluctuations in the vicinity of anticrossing. Otherwise, the elements are inhibited greatly. The results are attributed to the factors Γ_0, Γ_1, and Γ_2 shown in the inset. The electric field modulates the rotational states so that the redistributions of their wave functions effectively strengthen the correlation between two molecules. Improving the influence of the dipole-dipole interaction by the altered rotational states makes a significant impact on the magnitude of concurrence. Moreover, an increase in the parameter U_0 can equally enlarge the values of the elements. The concurrence is increased even when the electric field is tuned out of the anticrossing. Since it is different from the local modulation caused by the anticrossing, the influence of the parameter U_0 is much more extensive and leads to the result that the shape of the concurrence broadens in the case of large U_0.

Further analysis of concurrence is extended forward to the situations of the excited states. For the state j, the concurrence can be obtained by utilizing the density matrix $\rho = |\Phi_j\rangle\langle\Phi_j|$. The effect of temperature is eliminated. Note that the concurrence of the ground state $|\Phi_1\rangle$ coincides with the concurrence at $T = 0$ K. Figure 5 depicts the concurrences of the four states, depending on the electric field. When the field is away from the specific region, the effect of the dipole-dipole interaction becomes weak. The smooth energies of the states are observed in the inset. The concurrences of the states $|\Phi_2\rangle$ and $|\Phi_3\rangle$ are close to 1, while those of $|\Phi_1\rangle$ and $|\Phi_4\rangle$ are very small. In addition, the concurrence for $|\Phi_2\rangle$ is robust with the electric field. The result is similar to the case of free polar molecules [8]. However, the concurrences of the excited states $|\Phi_3\rangle$ and $|\Phi_4\rangle$ as well as $|\Phi_1\rangle$ undergo drastic changes in the region of anticossing. Because of the anticrossing, there are explicit variations in the energies of the states. Specifically, one can find that all of the concurrences show local maxima at the anticrossing point.

It is believed that the temperature strongly influences the entanglement of the system [22]. When the temperature rises, the population of the excited states becomes more significant. The ground state then mixes with the excited states [see Eq. (11)]. The dependence of temperature on the concurrence is illustrated in Fig. 6. The concurrence reveals decreasing behavior for different applied electric fields. The degree of decrease in concurrence at the anticrossing is larger than that seen in cases where $\omega \neq \omega^*$. This fact can be understood in light of the fact that the excited states as well as the ground state have relatively large concurrences at $\omega = \omega^*$ as shown in Fig. 5. The consequence of the mixing effect between these

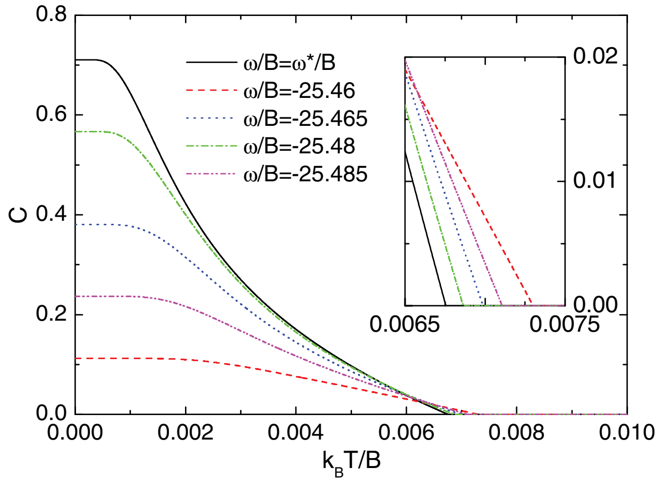

FIG. 6. (Color online) Temperature-dependent concurrence for $U_0/B = 0.01$. The inset emphatically shows the behavior of the concurrence $C \to 0$.

states makes the net concurrence smaller than that in the ground state. At a certain temperature, the concurrence eventually decreases to zero, where the entanglement of adsorbed-molecule system vanishes. The specific temperature depends on the electric field. More importantly, such a threshold temperature in the case of $\omega = \omega^*$ reaches the lowest point. As shown in the inset, the threshold value is $k_B T^*/B \simeq 6.76 \times 10^{-3}$ at $\omega = \omega^*$. Therefore, the anticrossing appearance accelerates to suppress the temperature-dependent concurrence.

IV. DISCUSSION

We briefly make some comparison with the related studies. The entanglement of a molecular system is probed by use of the rotational degrees of freedom [7,8]. Most efforts are concerned with free polar molecules, while we concentrate our study on the conical wells. The main difference comes from the presence of the quantum confinement. For polar molecules, the electric field is an effective tool to tailor the rotational properties [23–27]. The altered rotational states dominate the behavior of entanglement via a kind of correlation between polar molecules. In addition to the dipole-dipole interaction, the cavity is proposed to establish the correlation between molecules [6]. On the other hand, the adsorbed molecules manifest some interesting properties such as anticrossing features that are explicitly distinct from those of free molecules. The anticrossing-related phenomenons are similarly observed in various physics systems [28–30]. By controlling the electric field, the adsorbed-molecule system has significant entanglement with the help of the anticrossing. Such a consequence provides more insight into the underlying properties of entanglement based on the specific rotational states.

The confined molecules might be utilized as qubits and have potential applications to the field of quantum information processing. It is crucial to evaluate the performance of the qubit for realistic platforms [31]. As an example, a controlled-NOT gate based on the confined-molecule model is considered in the estimation. In order to implement the gate, one has to resolve the transitions $|00\rangle \leftrightarrow |01\rangle$ and $|10\rangle \leftrightarrow |11\rangle$ as well as the transitions $|00\rangle \leftrightarrow |10\rangle$ and $|01\rangle \leftrightarrow |11\rangle$ [8,9]. The gate time is approximately $\tau_g \sim 1/\nu$, where ν is the frequency difference between the transitions. On the contrary, spontaneous emission can destroy the coherence of the system, which limits the number of the qubit operations [7,32]. The corresponding coherence lifetime is estimated as $\tau_c \sim 3\pi\varepsilon_0\hbar^4 c^3/\mu^2\Delta^3$, where c is the speed of light and Δ is the energy difference between energy states. As the electric field is tuned around the region of the anticrossing, the related parameters are about $h\nu/B \lesssim 10^{-6}$ and $\Delta/B \lesssim 10^{-1}$. The LiH molecule of $B = 7.51\ \text{cm}^{-1}$ and $\mu = 5.88$ D are introduced into the calculation [33]. Accordingly, the gate time and coherence lifetime are $\tau_g \gtrsim 4 \times 10^{-6}$ s and $\tau_c \gtrsim 2 \times 10^5$ s, respectively. If the molecules are placed close to a dielectric surface, the lifetime τ_c' is modified to be lower than τ_c. In analogy to the atomic systems [34–36], the surface-induced effect is related to the refractive index. For silica, the ratio τ_c'/τ_g is obtained at approximately 10^{10}. On the other hand, a similar behavior exhibits in the case of the molecules near a metal surface. The lifetime is modified by the dielectric properties of the metal and the molecule-surface distance [36,37]. For example, the distance is set to be 10^{-6} m from the gold surface. The lifetime τ_c' is suppressed by two orders of magnitude relative to τ_c. By comparing the time scales, the gate time is much shorter than the different lifetimes in two situations. Therefore, one can conduct enough operations to achieve the specific computing work in the lifetime limit.

V. CONCLUSION

The entanglement of adsorbed-molecule system is studied in an electric field. The rotational states of adsorbed molecules can be modulated by tuning the electric field. In particular, the anticrossing features between the energy levels are observed in the presence of quantum confinement. This modulation on the rotational states varies the influence of the dipole-dipole interaction on the entanglement. In the vicinity of anticrossing, the concurrence exhibits an enhanced feature at zero temperature. In contrast, the temperature-dependent concurrence reveals a suppressed behavior at the anticrossing.

ACKNOWLEDGMENTS

This work is supported by the National Science Council of Taiwan under NSC Grants No. 97-2112-M-390-006-MY3 and No. 100-2112-M-390-002-MY3.

---

[1] L. Amico, R. Fazio, A. Osterloh, and V. Vedral, Rev. Mod. Phys. **80**, 517 (2008).

[2] R. Horodecki, P. Horodecki, M. Horodecki, and K. Horodecki, Rev. Mod. Phys. **81**, 865 (2009).

[3] B. Weber, H. P. Specht, T. Muller, J. Bochmann, M. Mucke, D. L. Moehring, and G. Rempe, Phys. Rev. Lett. **102**, 030501 (2009).

[4] N. Akopian, N. H. Lindner, E. Poem, Y. Berlatzky, J. Avron, D. Gershoni, B. D. Gerardot, and P. M. Petroff, Phys. Rev. Lett. **96**, 130501 (2006).
[5] C. L. Salter, R. M. Stevenson, I. Farrer, C. A. Nicoll, D. A. Ritchie, and A. J. Shields, Nature (London) **465**, 594 (2010).
[6] A. André, D. DeMille, J. M. Doyle, M. D. Lukin, S. E. Maxwell, P. Rabl, R. J. Schoelkopf, and P. Zoller, Nat. Phys. **2**, 636 (2006).
[7] E. Charron, P. Milman, A. Keller, and O. Atabek, Phys. Rev. A **75**, 033414 (2007).
[8] Q. Wei, S. Kais, B. Friedrich, and D. Herschbach, J. Chem. Phys. **134**, 124107 (2011).
[9] D. DeMille, Phys. Rev. Lett. **88**, 067901 (2002).
[10] S. F. Yelin, K. Kirby, and R. Côté, Phys. Rev. A **74**, 050301(R) (2006).
[11] L. Bomble, P. Pellegrini, P. Ghesquière, and M. Desouter-Lecomte, Phys. Rev. A **82**, 062323 (2010).
[12] Y. Y. Liao, Y. N. Chen, and D. S. Chuu, Chem. Phys. Lett. **398**, 418 (2004).
[13] K. Mishima and K. Yamashita, J. Chem. Phys. **130**, 034108 (2009).
[14] Q. Wei, S. Kais, and Y. P. Chen, J. Chem. Phys. **132**, 121104 (2010).
[15] P. Milman and A. Keller, Phys. Rev. A **79**, 052303 (2009).
[16] V. M. Rozenbaum, O. Ye. Vovchenko, and T. Ye. Korochkova, Phys. Rev. E **77**, 061111 (2008).
[17] J. W. Gadzuk, U. Landman, E. J. Kuster, C. L. Cleveland, and R. N. Barnett, Phys. Rev. Lett. **49**, 426 (1982).
[18] Y. Y. Liao, Y. N. Chen, W. C. Chou, and D. S. Chuu, Phys. Rev. B **73**, 115421 (2006).
[19] Y. T. Shih, Y. Y. Liao, and D. S. Chuu, Phys. Rev. B **68**, 075402 (2003).
[20] *Handbook of Mathematical Functions with Formulas, Graphs and Mathematical Tables*, edited by M. Abramowitz and I. A. Stegun (Dover, New York, 1965).
[21] W. K. Wootters, Phys. Rev. Lett. **80**, 2245 (1998).
[22] M. C. Arnesen, S. Bose, and V. Vedral, Phys. Rev. Lett. **87**, 017901 (2001).
[23] T. E. Wall, S. K. Tokunaga, E. A. Hinds, and M. R. Tarbutt, Phys. Rev. A **81**, 033414 (2010).
[24] M. Iñarrea, J. P. Salas, R. González-Férez, and P. Schmelcher, Phys. Lett. A **374**, 457 (2010).
[25] M. Lemeshko, M. Mustafa, S. Kais, and B. Friedrich, Phys. Rev. A **83**, 043415 (2011).
[26] Y. Y. Liao, Phys. Rev. B **83**, 115444 (2011).
[27] D. Townsend, B. J. Sussman, and A. Stolow, J. Phys. Chem. A **115**, 357 (2011).
[28] A. Nazir, B. W. Lovett, S. D. Barrett, J. H. Reina, and G. A. D. Briggs, Phys. Rev. B **71**, 045334 (2005).
[29] A. F. Slachmuylders, B. Partoens, F. M. Peeters, and W. Magnus, Appl. Phys. Lett. **92**, 083104 (2008).
[30] J. E. Rolon and S. E. Ulloa, Phys. Rev. B **82**, 115307 (2010).
[31] D. P. DiVincenzo, Fortschr. Phys. **48**, 771 (2000).
[32] K. Mishima and K. Yamashita, Chem. Phys. **361**, 106 (2009).
[33] M. Machholm and N. E. Henriksen, Phys. Rev. Lett. **87**, 193001 (2001).
[34] H. Khosravi and R. Loudon, Proc. R. Soc. London A **433**, 337 (1991).
[35] V. V. Ivanov, R. A. Cornelussen, H. B. van Linden van den Heuvell, and R. J. C. Spreeuw, J. Opt. B **6**, 454 (2004).
[36] M. S. Yeung and T. K. Gustafson, Phys. Rev. A **54**, 5227 (1996).
[37] S. Y. Buhmann, M. R. Tarbutt, S. Scheel, and E. A. Hinds, Phys. Rev. A **78**, 052901 (2008).